

Detecting defects in composite beams and plates using Bayesian inference

H. Chung¹, K. Lee¹

¹ School of Computer & Mathematical Sciences,
Auckland University of Technology, PB 92006 Auckland, New Zealand
e-mail: hchung@aut.ac.nz

Abstract

The topic of this paper is an inverse problem of identifying defects in composite beams and plates. The physical representation of defects is parametrized. Assuming Gaussian errors in measurements, the Bayesian inference is performed for those unknown parameters, and the most probable physical representations of defects are estimated. A composite beam/plate is usually made up of several layers, and there may be some defect in the bonding process or a defect may develop later. We use the natural frequencies of the beam/plate to estimate the position and the size of the defects. We propose that the bonding within the beam and plate can be modelled as added rigidity, which can be incorporated as an extra energy to the conventional strain energy. Standard Monte-Carlo simulation will then give the probabilistic properties of the natural frequencies of the beam/plate. The more prior information about the defects is limited, and thus we estimate the posterior distribution using the trans-dimensional Bayesian method, which lets us make an inference of different types of defects.

1 Introduction

Composite structures are made of two or more components to achieve stronger and lighter structures than they would be with a single component. In this paper, we study how to detect defects, particularly de-laminations, as an inverse problem. We consider a composite beam and a composite plate with two reinforcement beams. The beam is made up of two beams that are glued together, and the plate and the reinforcement beams are also glued together. A defect will be modelled as a de-lamination at the bonding-layer. The defects will be detected and estimated using the natural frequencies of the bending vibration. The bonding layer is modelled as extra layer of potential energy, in addition to the strain energy, required for the beam/plate to bend. This somewhat similar to the methods used in [1, 2], though the model here is simplified by omitting damping. As the beam bends, the bonding layer slips due to the discrepancy in the lateral displacement of the beams. Ideally there is no slippage and thus the bonding is perfect. Then the composite beam can simply be modelled as a single homogeneous elastic beam, and the composite plate can be modelled as a single plate with stiffeners. A de-lamination occurs when the bonding is not perfect.

The natural frequencies of the beam and the plate will be affected by the de-lamination (length and location) [3, 4, 5, 6, 7]. In other words, the eigenvalues of the linear system constructed for the bending motion will change as the lengths and the positions of the de-lamination changes. We will use this change in natural frequencies to estimate the de-lamination. This is slightly different from the methods of measuring the displacement at some positions at single or multiple frequencies, then formulating/solving the inverse problem as shown in [8, 9]. In practice the model or the forward problem is usually constructed using the Finite Element Analysis (FEA), then the measurements of structures with defect and without defect are compared to estimate the de-lamination (e.g., [3, 4]). Various methods of estimating defects are reviewed in

[6, 10], including inverse problems. In this paper, once the forward linear system is constructed for given de-laminations, an inverse problem can be constructed using Bayes' theorem. This method is relatively new in structural dynamics, though it has been used widely in the signal and image processing community for sometime. The inverse problem will be solved, i.e., the de-laminations are identified and estimated, using the Markov-Chain-Monte-Carlo method (MCMC). The initial data for the MCMC will be simulated from the forward problem solver with a Gaussian noise added to a set of natural frequencies. We will show that the forward problem solver here is so efficient that the MCMC can be performed within a reasonable amount of time.

The effectiveness or practicality of the MCMC depends on the efficiency of the forward problem solver, which is high in this case because of the modal representation rather than the finite element representation of the solution. The size of the linear system for the forward problem is much smaller here. It is however uncertain how valid the model for the bonding layer between components is. The evidence from [11] suggests that the slippage model is valid for wood-based composite structures with relatively low natural frequencies. It remains to be seen if this method can be scaled to smaller structures with higher natural frequencies.

In the following section, the method of solutions for the forward problem and the inverse problem will be shown. The mathematics of the method is not new, though the procedure to include the bonding layer slippage energy is a novelty of this method. In section 3, the numerical results of detections and estimation of the (multiple number of) lengths and positions of the de-laminations will be shown. The paper will be summarized in section 4.

2 Method of Solution

2.1 Forward problem

We first model a composite beam that is made up of two beams glued together. The schematics is shown in Fig. 1. Since the only the natural frequencies of the beams are considered here, the eigenvalue problem is formulated and solved for the clamped boundary conditions as depicted in Fig. 1.

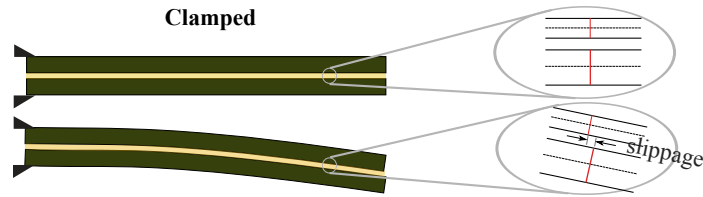


Figure 1: Schematic drawings of simply supported and clamped beam and their bending motion.

The bending motion of this Euler beams will be represented using the eigenfunctions of the motion, which satisfy the boundary conditions. We assume that there is no separation between the top and the bottom beams. The eigenfunctions of the clamped beam are

$$\psi_m(x) = \sqrt{\frac{1}{A}} [\cosh k_m x - \cos k_m x - \gamma_m (\sinh k_m x - \sin k_m x)], \quad m = 1, 2, \dots \quad (1)$$

where

$$\gamma_m = \frac{\cos k_m A + \cosh k_m A}{\sin k_m A - \sinh k_m A}$$

and the wavenumbers k_m are the roots of the frequency equation

$$\cos k_m A \cosh k_m A = -1$$

The vertical displacement of the beam can be expressed as

$$w(x) = \sum_{m=1}^N C_m \psi_m(x), \quad (2)$$

where C_m are the coefficients yet to be determined. See Fig. 2 for the coordinate system of the beam. The roots of this equation are found numerically, though $k_m \approx \pi(2m - 1)/2A$ for $m \geq 5$. Note that $\gamma_m \approx 1$ for $m \geq 5$.

The second case of the forward problem is a beam-reinforced plate as shown in Fig. 3. The clamped edge again breaks the symmetry of the position of the defects. Figure 3 shows the coordinate system for the model. Only the vertical bending motion will be considered here, and thus the torsional and the in-plane deflections will not be included in the model. The eigenfunctions for the plate are

$$w_{mn}(x, y) = \psi_m(x)\phi_n(y), \quad m, n = 1, 2, \dots \quad (3)$$

where ϕ_n is the eigenfunctions for the y -direction when the boundary $y = 0$ is clamped (see to Eq. (1)). Then the vertical displacement of the plate is given by

$$w(x, y) = \sum_{m=1}^M \sum_{n=1}^N C_{mn} \psi_m(x)\phi_n(y), \quad (4)$$

Note that the number of terms is truncated for later numerical computation, and the terms for the plate in the x and y directions need not be the same.

In both plate and beam cases, we assume that there is a thin layer of contact between two beams and plate and beams. The defects will occur in this layer. The defects will affect the total stiffness matrix of the structure, and thus change the natural frequencies. The stiffness matrix will be derived from the strain energy and the energy required for the slippage in the mid-layer.



Figure 2: Axis orientation of the composite beam with one clamped edge at $x = 0$.

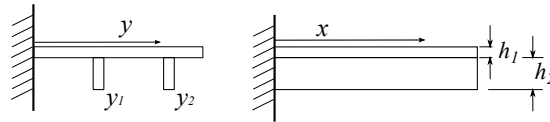


Figure 3: Axis orientation of the beam-reinforced plate (not to scale) with two clamped edges at $x = 0$ and $y = 0$. The beams are running along the x -axis.

The energy of the harmonic vibration of a beam and a plate can be expressed using only the function of the displacement, which are $w(x)$ for the beam and $w(x, y)$ for the plate. The strain energy for a beam ([12]) is

$$U_b = \frac{EI}{2} \int_0^A (w''(x))^2 dx \quad (5)$$

where E is Young's modulus and I is moment of inertia, which, for example, is calculated by $I = h_3 h_1^3 / 12$, h_3 being the width of the beam for the top beam. The strain energy of the composite beam will be sum of

the two beams. The strain energy of a plate is

$$U_p = \frac{D}{2} \int_0^A \int_0^B \{(\nabla^2 w)^2 + 2(1 - \nu) [w_{xy}^2 - w_{xx}w_{yy}]\} dx dy \quad (6)$$

where the bending stiffness D is calculated by $D = Eh_1^3/12(1 - \nu^2)$ for the thickness h_1 and Poisson ratio ν . The strain energy of the reinforcement beams are given by

$$U_{rb} = \frac{EI}{2} \sum_{j=1}^J \int_0^A (w''(x, y_j))^2 dx \quad (7)$$

where the position of the beams are denoted by $y = y_j, j = 1, 2, \dots, J$. The additional energy due to the slippage in the contact layer [11] is given by

$$U_s = \frac{s}{2} \sum_{j=1}^J \int_0^A ((h_1 w_x(x, y_j) + h_2 w_x(x, y_j))^2 dx \quad (8)$$

where s denotes the slippage constant. The modelling regime for the slippage energy is depicted in Fig. 1, which shows the discrepancy in the lateral displacement as the beams bend. The de-lamination is modelled as zero-slippage resistance, which is defined as $[c_i - l_i, c_i + l_i], i = 1, 2, \dots, N_d$ where c_i is the centre of the de-lamination, $2l_i$ is the width and N_d is the number of defects. Then the integral in Eq. (8) becomes

$$U_s = \frac{s}{2} \sum_{j=1}^J \int_{\mathcal{D}} ((h_1 w_x(x, y_j) + h_2 w_x(x, y_j))^2 dx$$

where \mathcal{D} is the integral limit which has the de-lamination regions subtracted.

The linear system can now be formulated for the coefficients of the eigenfunction expansion of the deflection $w(x)$ or $w(x, y)$ in Eqs. (2) and (4), respectively. The linear systems are derived for the vectors

$$\mathbf{c} = \begin{pmatrix} C_1 \\ C_2 \\ \vdots \\ C_M \end{pmatrix}, \quad \text{or} \quad \mathbf{c} = \begin{pmatrix} C_{11} \\ C_{12} \\ \vdots \\ C_{MN} \end{pmatrix}$$

Then, the eigenvalue problem is given by

$$\mathcal{M}^{-1} \mathcal{U} \mathbf{c} - (2\pi f)^2 \mathbf{c} = 0 \quad (9)$$

where \mathcal{M} and \mathcal{U} are the mass density and stiffness matrices, and $(2\pi f)^2$ is the eigenvalue, in other words f is the natural frequency.

The matrix for the eigenvalue problem can be constructed using Eqs. (5) to (8). Hence, the matrix for the beam case is

$$\mathcal{U}_b = \begin{pmatrix} EI_1 k_1^4 & 0 & \dots & 0 \\ 0 & EI_1 k_2^4 & & 0 \\ \vdots & & \ddots & \vdots \\ 0 & 0 & \dots & EI_1 k_M^4 \end{pmatrix} + \begin{pmatrix} EI_2 k_1^4 & 0 & \dots & 0 \\ 0 & EI_2 k_2^4 & & 0 \\ \vdots & & \ddots & \vdots \\ 0 & 0 & \dots & EI_2 k_M^4 \end{pmatrix} \quad (10)$$

where I_1 and I_2 are moment of inertia for the top and bottom beams, respectively. The stiffness matrix for the plate with the reinforcement beams is

$$\mathcal{U}_p = \begin{pmatrix} D(k_1^2 + \kappa_1^2)^2 & 0 & \dots & 0 \\ 0 & D(k_2^2 + \kappa_1^2)^2 & & 0 \\ \vdots & & \ddots & \vdots \\ 0 & 0 & \dots & D(k_M^2 + \kappa_N^2)^2 \end{pmatrix} + T^t \begin{pmatrix} EI_2 k_1^4 & 0 & \dots & 0 \\ 0 & EI_2 k_2^4 & & 0 \\ \vdots & & \ddots & \vdots \\ 0 & 0 & \dots & EI_2 k_M^4 \end{pmatrix} T$$

where the matrix T represents the linear operation on the vector \mathbf{c} , and the m 'th element of the vector $T\mathbf{c}$ is given by

$$[T\mathbf{c}]_m = \sum_{n=1}^N C_{mn} \phi_n(y_j)$$

The stiffness matrix \mathcal{U} for the beam or the plate in Eq. 9 can be derived by summing all the energy matrices,

$$\mathcal{U} = \mathcal{U}_b + \mathcal{U}_s \quad \text{or for the plate} \quad \mathcal{U} = \mathcal{U}_p + \mathcal{U}_s$$

For the composite beam, the mass density matrix is simply a diagonal matrix of the mass density of the beam. For the composite plate the matrix \mathcal{M} is given by $\mathcal{M}_p + T^t \mathcal{M}_b T$, where \mathcal{M}_b and \mathcal{M}_p are diagonal matrices of the mass density of the beams and plate, respectively.

The natural frequencies of the linear system given by Eq. 9 can be computed using any elimination algorithm. In this case, MatLab is used to compute the natural frequencies, which takes a short amount of time. We note that we set $M = 20$ and $N = 4$ and the size of the linear system for the beam was 20×20 and for the plate was 80×80 .

2.2 Inverse problem

We suppose that there are N_d -number of defects on the composite beam/beam-reinforced plate. The defect is defined by a position and a length, denoted by c and l , respectively. Here, l is a half length of the defect and a range of the defect is $[c - l, c + l]$. When all defects, $\{c_j, l_j\}_{j=1}^{N_d}$, are known, the first N_f exact natural frequencies, denoted by μ_1, \dots, μ_{N_f} , are computed using the forward map described in section 2.1. The inverse problem is a procedure that finds the defects from the observed natural frequencies, which consist of random noise.

We use the Bayesian inference to estimate the distribution for unknown defects, $\{c_j, l_j\}_{j=1}^{N_d}$, from an observed set of natural frequencies, $\{f_i\}_{i=1}^{N_f}$. This is called the posterior distribution and denoted by $p(c_1, \dots, c_{N_d}, l_1, \dots, l_{N_d} | \{f_i\}_{i=1}^{N_f})$. If probability for $\{f_i\}_{i=1}^{N_f}$ is non-zero, the posterior is represented by the Bayes' rule, which is

$$\begin{aligned} p(c_1, \dots, c_{N_d}, l_1, \dots, l_{N_d} | \{f_i\}_{i=1}^{N_f}) &= \frac{p(\{f_i\}_{i=1}^{N_f} | c_1, \dots, c_{N_d}, l_1, \dots, l_{N_d}) p(c_1, \dots, c_{N_d}, l_1, \dots, l_{N_d})}{p(\{f_i\}_{i=1}^{N_f})} \\ &\propto p(f | c_1, \dots, c_{N_d}, l_1, \dots, l_{N_d}) p(c_1, \dots, c_{N_d}, l_1, \dots, l_{N_d}). \end{aligned} \quad (11)$$

where $p(f | c_1, \dots, c_{N_d}, l_1, \dots, l_{N_d})$ is the likelihood and $p(c_1, \dots, c_{N_d}, l_1, \dots, l_{N_d})$ is a prior. The posterior distribution is proportional to the likelihood and prior.

Because of the assumption that a Gaussian random noise is in the natural frequency observation, the i -th observation f_i is normally distributed with the mean of μ_i and standard deviation of σ_i ,

$$p(f_i | \mu_i, \sigma_i^2) = \frac{1}{\sqrt{2\pi\sigma_i^2}} e^{-(f_i - \mu_i)^2 / 2\sigma_i^2}, \quad i = 1, \dots, N_f. \quad (12)$$

Here, the standard deviation σ_i represents the noise error level and a relative error μ_i is chosen for the simulations in section 3. The likelihood in Eqs. (11) is assessed by a probability of f conditioned on using the exact natural frequency, μ , in which is computed for a given defect

$$p(\{f_i\}_{i=1}^{N_f} | c_1, \dots, c_{N_d}, l_1, \dots, l_{N_d}) = \prod_{i=1}^{N_f} \frac{1}{\sqrt{2\pi\sigma_i^2}} e^{-(f_i - \mu_i)^2 / 2\sigma_i^2}. \quad (13)$$

We assume that all defects are within the beam with the length of A and neighbouring defects do not overlap. The domain for defect is $(c, l) \in [0, A] \times [0, A/2]/\text{overlapping}$. The prior is formulated as the following.

$$\begin{aligned} p(c_1, \dots, c_{N_d}, l_1, \dots, l_{N_d}) &= \mathbb{1}(N_{\text{overlap}} = 0) \prod_{j=1}^{N_d} p(c_j)p(l_j) \\ &= \mathbb{1}(N_{\text{overlap}} = 0) \prod_{j=1}^{N_d} U(c_j|0, A)U(l_j|0, A/2) \end{aligned} \quad (14)$$

where N_{overlap} is a number of overlapping defects. If none of defect overlap, $\mathbb{1}(N_{\text{overlap}} = 0) = 1$. Otherwise $\mathbb{1}(N_{\text{overlap}} = 0) = 0$. The uniform distribution, U , is used for both $p(c)$ and $p(l)$ in Eq. (14). Although a simple uniform prior is used here, a more informative prior could be considered for more complex problems.

The posterior given by Eq. (11) is found using the likelihood (Eq. (13)) and the prior (Eq. (14)). The analytical formula for the posterior is not available for this problem and thus the MCMC method is used to simulated the posterior numerically. A sequence of random samples from the posterior is simulated using the Metropolis Hastings algorithm and those samples contain the Markov chain property.

The Markov chain with the length of T is denoted by $\{c_1^{(t)}, \dots, c_{N_d}^{(t)}, l_1^{(t)}, \dots, l_{N_d}^{(t)}\}_{t=1}^T$. At each iteration, a sample $\{c_j, l_j\}_{j=1}^{N_d}$ is generated by sampling (c_j, l_j) for each defect in turn. At t -th iteration, with a given $\{c_j^{(t-1)}, l_j^{(t-1)}\}_{j=1}^{N_d}$, a sample $\{c_j^{(t)}, l_j^{(t)}\}_{j=1}^{N_d}$ is generated by the following algorithm.

Step 1 Set $j = 1$.

Step 2 Generate the proposals, $c^* \sim q(\cdot|c_j^{(t-1)})$ and $l^* \sim q(\cdot|l_j^{(t-1)})$.

Step 3 Set the vectors

$$c^0 = c' = [c_1^{(t)}, \dots, c_{j-1}^{(t)}, c_j^{(t-1)}, \dots, c_{N_d}^{(t-1)}]$$

and

$$l^0 = l' = [l_1^{(t)}, \dots, l_{j-1}^{(t)}, l_j^{(t-1)}, \dots, l_{N_d}^{(t-1)}].$$

Replace the j -th element in c' and l' to $c'_j = c^*$ and $l'_j = l^*$.

Step 4 Compute the prior $p(c', l')$ in Eq. (14) and likelihood $p(f|c', l')$ in Eq. (13) for c' and l' .

Step 5 Compute the acceptance probability, $\alpha(c^*, l^*|c_j^{(t-1)}, l_j^{(t-1)})$

$$\alpha(c^*, l^*|c_j^{(t-1)}, l_j^{(t-1)}) = \min \left(1, \frac{p(f|c', l')p(c', l')q(c_j^{(t-1)}|c^*)q(l_j^{(t-1)}|l^*)}{p(f|c^0, l^0)p(c^0, l^0)q(c^*|c_j^{(t-1)})q(l^*|l_j^{(t-1)})} \right).$$

Step 6 Accept c^* and l^* with $\alpha(c^*, l^*|c_j^{(t-1)}, l_j^{(t-1)})$. If they are accepted, set $c_j^{(t)} = c^*$ and $l_j^{(t)} = l^*$. Otherwise $c_j^{(t)} = c_j^{(t-1)}$ and $l_j^{(t)} = l_j^{(t-1)}$.

Step 7 Set $j = j + 1$ and repeat the Steps 2 – 6 until $j = N_d$.

In this paper, the proposal density q is the normal distribution with a mean of the condition and variance of φ^2 ;

$$q(c^*|c_j^{(t-1)}) = N(c^*|c_j^{(t-1)}, \varphi_c^2), \text{ and } q(l^*|l_j^{(t-1)}) = N(l^*|l_j^{(t-1)}, \varphi_l^2), \quad j = 1, \dots, N_d$$

These are also called the normal random walk proposals. The variances φ_c^2 and φ_l^2 are related to the random walk sizes. When a size of walk is too big, proposals are hardly accepted. For a very small walk size, the

chain takes very long to explore the posterior state space. For our simulation studies in the following section, the number of unknown parameters are relatively small and φ_c^2 and φ_l^2 are manually adjusted following [13]. The adaptive MCMC [14] can be easily adapted to this algorithm and a random walk size is adaptively tuned. This approach is particularly useful as the dimension of posterior (a number of unknown parameters) increases. Broad studies on MCMC method up to recent is well summarized in [15].

3 Numerical Results

The physical and material parameters for the beam and the plate are given in Table 1. The material parameters are those of typical wood panels and beams. Note that all parameters are measurable except the slippage constant, which needs to be determined by modelling and parameter fitting.

	notation	value
length	A	1.5 m
width	B	0.3 m
mass density	m	500 kgm ⁻³
Young's modulus	E	14 GPa
thickness	h_1	0.01 m
thickness	h_2	0.1 m
beam width	h_3	0.05 m
Poisson ratio	ν	0.4
slippage constant	s	10 ⁸ Nm ⁻¹
location of the beams	y_1, y_2	0.15 m, 0.25 m

Table 1: Notations and values of the physical parameters

For the simulation study, the following four cases are considered.

- A composite beam with one defect.
- A composite beam with two defects.
- A composite beam with three defects.
- A beam-reinforced plate with one defect on each beam.

For each model, a set of natural frequencies, $\{f_i\}_{i=1,2,\dots,N_f}$, is generated by adding a Gaussian noise to the exact natural frequency $\{\mu_i\}_{i=1,2,\dots,N_f}$. For the numerical computation, we set $N_f = 10$ for the beam and $N_f = 20$ for the plate. The first 10 natural frequencies for the beam range approximately from 150 Hz to 10 kHz. The first 20 natural frequencies for the plate range approximately from 130 Hz to 2.5 kHz. The Gaussian noise here is generated by a zero-mean normal distribution with the standard deviation, σ_i for each i . Here, σ_i is 0.5% of μ_i . We estimate the posterior distribution for $\{c_j, l_j\}_{j=1}^{N_d}$ using the MCMC method. The Markov chain with the length of 10^5 is simulated and the first 2,000 iterations are ignored for the inference.

The means and 95% confidence intervals for $\{c_j, l_j\}_{j=1}^{N_d}$ are shown in Table 2. In general, the true positions and length values are within the 95% confidence intervals and the defects are identified well. This is supported graphically by the marginal posterior distributions in Figs. 4 – 7. Uni-modal marginal posterior distributions are centred at near the true values and thus the data is informative of the defects.

In the case of three defects, one defect is estimated with a relatively wider range, which affects the rest estimates of the other defects. We speculate that the defect near the clamped edge has less effects on the natural frequencies than the other defects because the displacement near the clamped edge is small. However we have noticed that the method performs well when there is a single defect near the edge.

Model	Parameter	Mean	95% confidence interval	True value
One defect	Position (c)	0.9882	[0.9382 , 1.0324]	1
	Length (l)	0.0337	[0.0266 , 0.0407]	0.035
Two defects	Position (c)	0.5023	[0.4625 , 0.5495]	0.5
		0.9856	[0.9301 , 1.0327]	1
	Length (l)	0.0341	[0.0253 , 0.0421]	0.035
		0.0346	[0.0254 , 0.0437]	0.035
Three defects	Position (c)	0.3582	[0.0628 , 0.6902]	0.3
		0.7294	[0.6691 , 0.7917]	0.75
		1.1925	[1.1637 , 1.2257]	1.2
	Length (l)	0.0171	[0.0008 , 0.0402]	0.035
		0.0444	[0.0175 , 0.0603]	0.035
		0.0399	[0.0288 , 0.0503]	0.035
Plate	Position (c)	0.6085	[0.5564 , 0.6723]	0.6
		0.9823	[0.9494 , 1.0161]	1
	Length (l)	0.0354	[0.0235 , 0.0475]	0.05
		0.0528	[0.0473 , 0.0582]	0.05

Table 2: Parameter estimate result using the MCMC method.

A trace plot is often used as a graphical tool to monitor the convergence of the simulated Markov chain. All simulated chains were monitored graphically and converged to the target distributions. For example, Fig. 8 shows the convergence of a simulated chain for the composite beam with one defect.

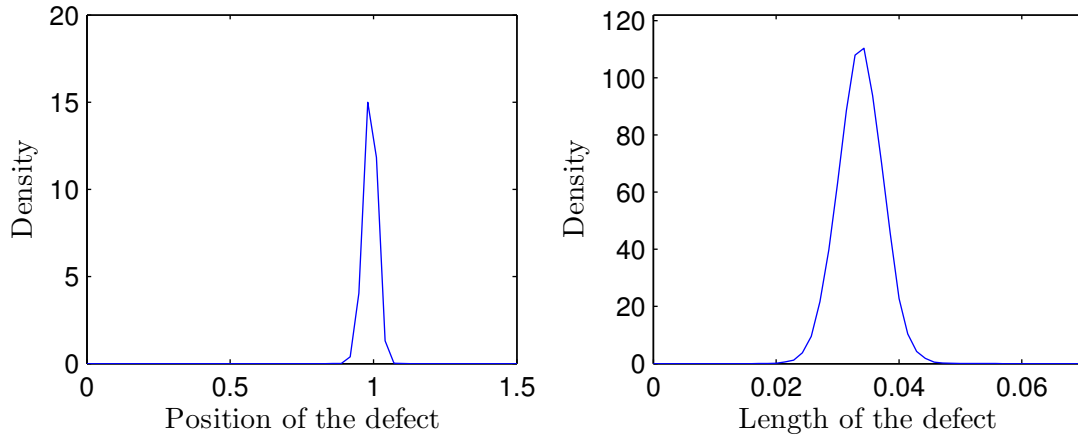


Figure 4: Marginal posterior distributions for the position (c) and length (l) parameters for the composite beam with one defect.

4 Summary

In this paper the Bayes' theorem is implemented using the MCMC to solve the inverse problem of estimating the position and the length of de-laminations in composite beam and plate. The method uses the natural frequencies of the structures to estimate the de-laminations. The natural frequencies are computed using the eigenfunction expansion of the bending vibration of the structures, and thus the computation of the natural frequencies takes short time. The numerical results of MCMC show that a single defect in a composite beam can be estimated accurately. The accuracy of the de-lamination near the clamped edge is lower than others.

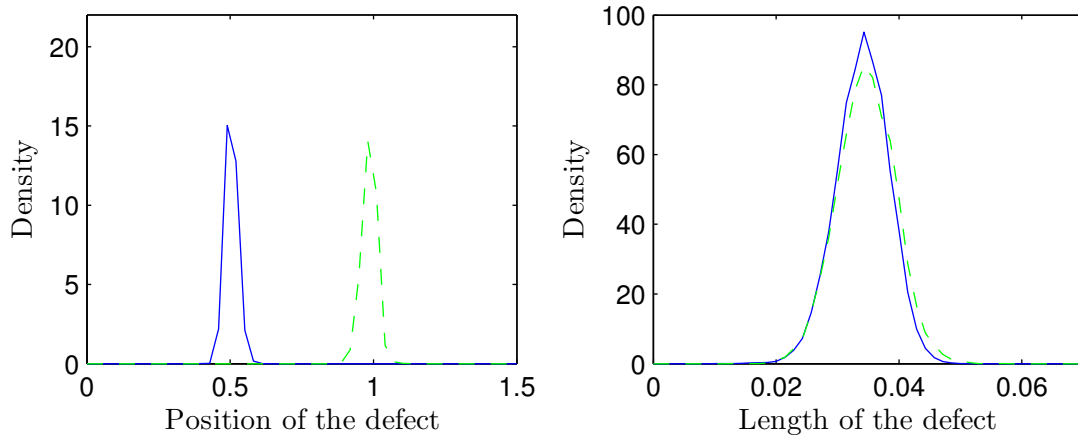


Figure 5: Marginal posterior distributions for the position (c) and length (l) for the composite beam with two defects. The solid and dashed lines respectively represent the distributions for parameters for each defect.

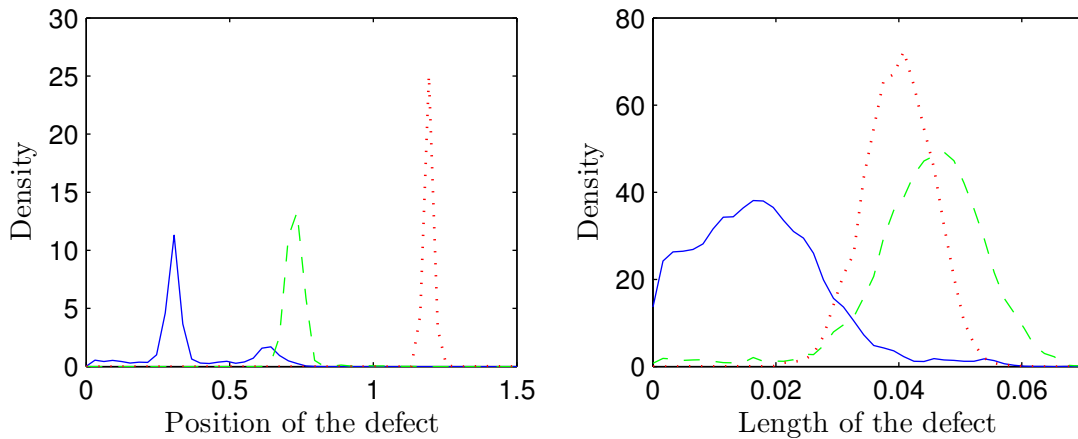


Figure 6: Marginal posterior distributions for the position (c) and length (l) for the composite beam with three defects. The solid and dashed lines respectively represent the distributions for parameters associated with each defect.

The de-laminations in composite plate are more difficult to estimate, though the positions are estimated accurately. The estimates of the length of the de-lamination show certain bias either to larger or smaller values. The reason is yet unknown to the authors. In all cases, the MCMC chains converge within 2000 iterations, which require short length of computing time and enough for determining the positions and the lengths of the de-lamination. We note that many more iterations are required to construct smooth probability distribution of the de-laminations. Further study is needed for determining the effectiveness of the method for structures with higher or lower natural frequencies. It remains to be seen how the results in this paper can be scaled to other materials and sizes. As shown in section 2, the method here assumes that we know the number of de-laminations. If we assume no such priori information, the MCMC simulation would take much longer. A further study is needed for effective method of estimating the number of de-laminations in addition to lengths and positions.

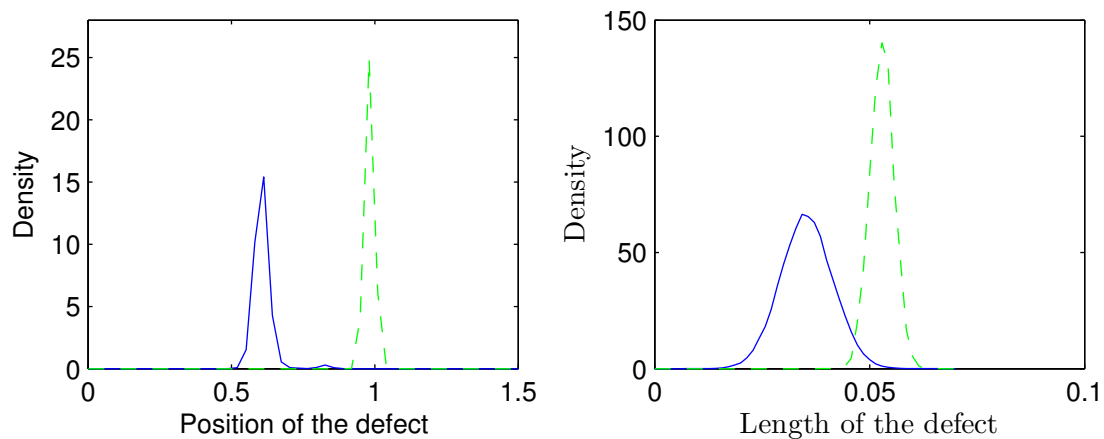


Figure 7: Marginal posterior distributions for the position (c) and length (l) parameters for the composite plate with one defect on each beam. The solid and dashed lines respectively represent the distributions for parameters associated with a defect in each beam.

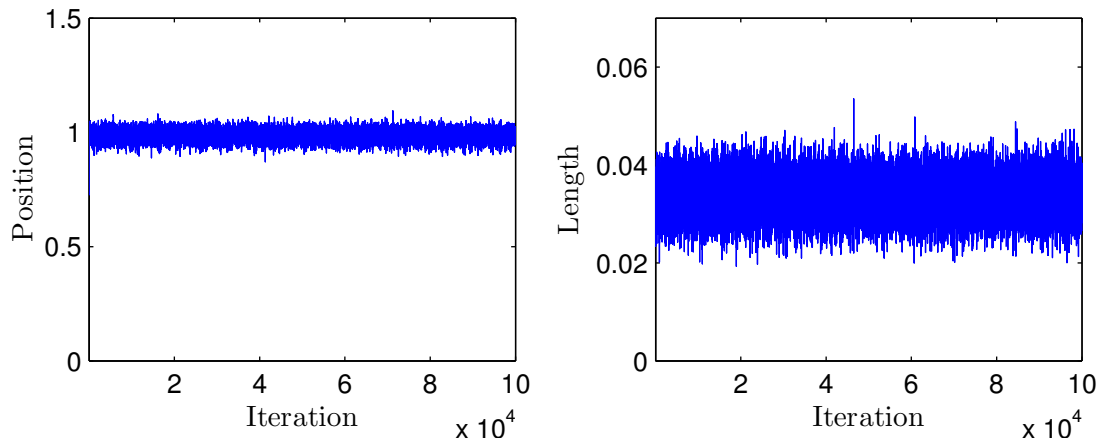


Figure 8: Trace plots of simulated Markov chains for the position (left) (c) and length (right) (l) for the composite beam with one defect.

References

- [1] B. Mace, *Damping of beam vibrations by means of a thin constrained viscoelastic layer: evaluation of a new theory*, Journal of Sound and Vibration, Vol. 172, No. 5 (1994), pp. 577–591
- [2] H. V. Vu, A. M. Ordóñez and B. H. Karnopp, *Vibration of a double-beam system*, Journal of Sound and Vibration, Vol. 229, No. 4 (2000), pp. 807–822
- [3] P. Cawley and R. Adams, *The location of defects in structures from measurements of natural frequencies*, The Journal of Strain Analysis for Engineering Design, Vol. 14, No. 2 (1979), pp. 49–57.
- [4] A. Paolozzi and I. Peroni, *Detection of debonding damage in a composite plate through natural frequency variations*, Journal of Reinforced Plastics and Composites, Vol. 9, No. 4 (1990), pp. 369–389.
- [5] Y. Shi, H. Sol, and H. Hua, *Material parameter identification of sandwich beams by an inverse method*, Journal of Sound and Vibration, Vol. 290, No. 3 (2006), pp. 1234–1255.

- [6] M. I. Friswell, *Damage identification using inverse methods*, Philosophical Transactions of the Royal Society A: Mathematical, Physical and Engineering Sciences, Vol. 365, No. 1851 (2007), pp. 393–410.
- [7] R. Loendersloot, T. Ooijevaar, L. Warnet, A. d. Boer, and R. Akkerman, *Vibration based structural health monitoring of a composite plate with stiffeners*, in *USD2010 international conference on uncertainty in structural dynamics*, Leuven (2010), pp. 909–924.
- [8] Y. Zou, L. Tong, and G. Steven, *Vibration-based model-dependent damage (delamination) identification and health monitoring for composite structures a review*, Journal of Sound and vibration, Vol. 230, No. 2 (2000), pp. 357–378.
- [9] C. Lecomte, B. Mace, J. Forster, and N. Ferguson, *Bayesian localisation of damage in a linear dynamic system*, in *USD2010 international conference on uncertainty in structural dynamics*, Leuven (2010), pp. 4953–4964.
- [10] S. S. Kessler, S. M. Spearing, M. J. Atalla, C. E. Cesnik, and C. Soutis, *Damage detection in composite materials using frequency response methods*, Composites Part B: Engineering, Vol. 33, No. 1 (2002), pp. 87–95.
- [11] H. Chung and G. Emms, *Fourier series solutions to the vibration of rectangular lightweight floor/ceiling structures*, Acta Acustica United With Acustica, Vol. 94 (2008), pp. 401–409.
- [12] I. Shames and C. Dym, *Energy and finite element methods in structural mechanics*. New York: Taylor & Francis, SI units ed., (1991).
- [13] A. Gelman, G. Roberts, and W. Gilks, *Efficient Metropolis jumping rules*, in *Bayesian Statistics 5* (J. Bernardo, J. Berger, A. Dawid, and A. Smith, eds.), pp. 559–607, Oxford University Press (1996).
- [14] G. Roberts and J. Rosenthal, *Optimal scaling for various Metropolis-Hastings algorithms*, Statistical Science, Vol. 16, No. 4 (2001), pp. 312–390.
- [15] S. Brooks, A. Gelman, G. Jones, and X. Meng, eds., *Handbook of Markov chain Monte Carlo*. Chapman & Hall/CRC Handbooks of Modern Statistical Methods, Chapman and Hall/CRC, 1 ed., (2011).